

Numerical study of the error sources in the experimental estimation of thermal diffusivity: an application to debris-covered glaciers

Calvin Beck^{1,2} and Lindsey Nicholson²

¹Normandie Université – UNICAEN - UNIROUEN, CNRS, UMR 6143 M2C, Laboratoire Morphodynamique Continentale et Côtière, Caen, France

²Department of Atmospheric and Cryospheric Sciences, University of Innsbruck, Innsbruck, Austria

Correspondence: Calvin Beck (calvin.beck@unicaen.fr)

Abstract. In tectonically active mountain regions, the thinning of alpine glaciers due to climate change favors the development of debris-covered glaciers. A surface debris layer significantly modifies a glacier's melt and therefore modifies its evolution. The melt modification is primarily dependent on the thermal resistance of the debris cover, with thermal resistance being a function of debris thickness and effective thermal conductivity. The most commonly used method to calculate apparent thermal diffusivity of supraglacial debris layers is based on heat diffusion principles and an estimate of volumetric heat capacity of the debris as presented by Conway and Rasmussen (2000) using a vertical array of temperature measurements through the supraglacial debris cover. This study explores the effect of the temporal and spatial sampling interval, and instrument discretization on the thermal diffusivity values derived using this method. We show that increasing temporal and spatial sampling intervals increase truncation errors and therefore systematically underestimate calculated values of thermal diffusivity. The thermistor discretization, the shape of the diurnal temperature cycle, and misrepresenting the vertical thermistor position also result in systematic errors. We provide an interactive analysis tool and best practice guidelines to help researchers investigate the effect of the sampling interval on calculated sub-debris ice melt and plan future measurement campaigns.

1 Introduction

Debris-covered glaciers can be found in tectonically active mountain regions such as Alaska, the European Alps, High Mountain Asia, or New Zealand (Herreid and Pellicciotti, 2020), where large amounts of debris migrate into the ice via glacial and periglacial processes (Shugar and Clague, 2011; Scherler et al., 2018; Anderson et al., 2018). Rock debris can be sourced from basal or sub aerial erosion from the surrounding terrain. Debris falling onto the ablation zone contributes directly to any surface debris load, but debris added to the glacier surface in the accumulation zone or sourced subglacially is transported englacially to the ablation area of the glacier, where it melts out to form a new supraglacial debris cover or thickens the existing surface debris (Nicholson and Benn, 2006; Kirkbride and Deline, 2013; Anderson et al., 2018), as shown in Figure 1a. Herreid and Pellicciotti (2020) show that $7.3 \pm 3.3\%$ of all mountain-glacier area is covered by a rock debris cover, but this surface area is expected to increase in absolute and percentage terms in the future with continued glacier decline (Deline and Orombelli, 2005; Kellerer-Pirklbauer et al., 2008; Quincey and Glasser, 2009; Bhambri et al., 2011; Bolch et al., 2012; Kirkbride and Deline, 2013; Thakuri et al., 2014; Scherler et al., 2018; Tielidze et al., 2020). As surface debris significantly modifies the glacier

25 evolution and runoff over time (Østrem, 1959; Rowan et al., 2015; Huo et al., 2021; Mayer and Licciulli, 2021; Nicholson et al., 2021; Rounce et al., 2023), the impact of debris-covered areas is expected to become more relevant in future runoff and glacier change projections (Rounce et al., 2015).

In comparison to clean ice, thin or patchy debris amplifies ice melt due to its higher absorptivity of short-wave radiation while thicker debris layers reduce ice melt due to the insulation and attenuation of the diurnal heating signal (Inoue and Yoshida, 30 1980; Kayastha et al., 2000; Kirkbride and Dugmore, 2003; Mihalcea et al., 2006; Brock et al., 2010; Reznichenko et al., 2010; Fyffe et al., 2014; Minora et al., 2015). The relationship between debris thickness and ablation rate varies for different debris layer compositions and prevailing climatological conditions but retains the same character (Fig. 1b) with the critical debris thickness beyond which sub-debris ice ablation is inhibited compared to clean ice ablation ranging from 15 to 115 mm (Østrem, 1959; Mattson, 1993; Nicholson and Benn, 2006) dependent on the debris optical and thermal properties and the ambient 35 climate (Inoue and Yoshida, 1980; Nakawo and Takahashi, 1982; Adhikary et al., 1997; Reznichenko et al., 2010). Therefore, in contrast to clean ice glaciers, where the melt increases towards the glacier tongue in response to typical environmental temperature lapse rates, the spatial pattern of melt of debris-covered glaciers depends more on the debris thickness than on the elevation (e.g. Benn et al., 2012; Rowan et al., 2021; Nicholson et al., 2021). Globally, the effect of surface debris is to delay the loss of debris-covered glacier termini, highlighting the need to accurately incorporate its insulating effects in glacier 40 projections for the coming decades (Rounce et al., 2023).

Although under certain circumstances heat can be transferred through the debris by convection, advection, and radiation, observations (e.g. Conway and Rasmussen, 2000; Nicholson and Benn, 2012) show that the system often, and especially under dry stable conditions, approximates Fourier's law of conduction $q = -k\nabla T$, where q represents the local heat flux density, k the thermal conductivity, and T the temperature (Fourier, 1955; Cannon, 1984). Consequently, for horizontally homogeneous 45 debris layers the one-dimensional heat conduction equation for a homogeneous, isotropic medium (Eq. 1) has been used to derive the apparent thermal diffusivity, κ , from the spatio-temporal variation of a vertical profile of temperature measurements, by finding the gradient of the regression line between the first derivative of temperature with time and the second derivative of temperature with depth. Apparent thermal conductivity k can then be calculated from κ and the volumetric heat capacity of the debris, given by the specific heat capacity c_s and the material density ρ (Eq. 2).

$$50 \quad \frac{\partial T}{\partial t} = \kappa \frac{\partial^2 T}{\partial x^2} + \text{const.} \quad (1)$$

$$\kappa = \frac{k}{\rho \cdot c_s} \quad \begin{array}{l} \leftarrow \text{thermal conductivity} \\ \leftarrow \text{heat capacity} \end{array} \quad (2)$$

This method of determining debris apparent thermal conductivity was presented by Conway and Rasmussen (2000) and has been widely used (e.g. Nicholson and Benn, 2006; Haidong et al., 2006; Juen et al., 2013; Chand and Kayastha, 2018; Rounce 55 et al., 2015; Rowan et al., 2021), becoming the standard method for determining the value of debris thermal conductivity to

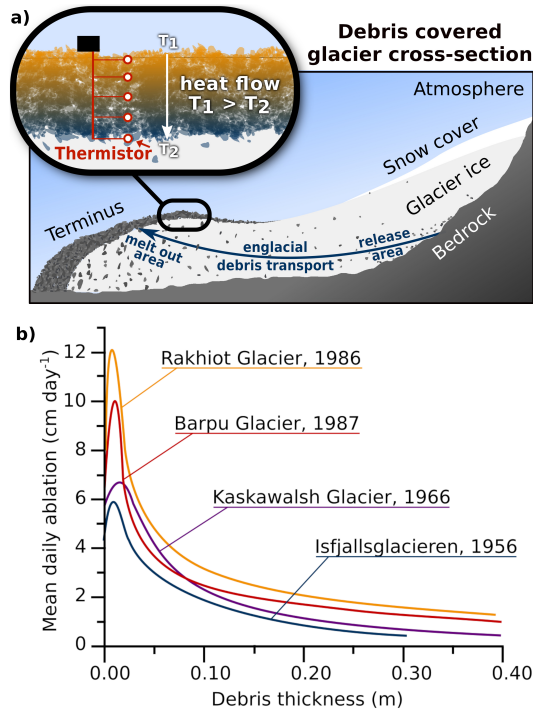


Figure 1. a) Schematic of a debris-covered glacier with debris transport of subglacially sourced rock debris from release area to melt out area. The inset shows a classical thermal diffusivity measurement site, consisting of thermistors at several heights between the near-surface and the debris-ice interface. b) Measurements of the so-called Østrem curves for different glaciers show a common pattern of variation of daily melt rate versus the debris depth, with site-specific variations in maximum ablation and the debris thickness associated with it. Redrawn from Mattson (1993).

be used in surface energy models accounting for supraglacial debris (Reid and Brock, 2010; Fyffe et al., 2014; Evatt et al., 2015). Application of this method requires a vertical array of temperature measurements through the supraglacial debris cover (Fig. 1a) for conditions in which the debris heat transfer closely approximates that of a conductive system, and an estimate of the volumetric heat capacity of the debris. Evidence of linear mean multi-day temperature profiles under stably oscillating surface forcing conditions suggest that the application of Eq. 1 to supraglacial debris is generally justifiable (Conway and Rasmussen, 2000; Rowan et al., 2021), although we note that non-conductive processes can be significant during seasonal change and water percolation (e.g. Nicholson and Benn, 2012).

In some cases, analysis of field data to determine apparent thermal diffusivity at several levels within the debris cover, rather than as a bulk analysis over all depths, reveals vertical variation in thermal properties, consistent with stratification of grain size and water content observed in natural debris covers and/or depth-dependent contributions from non-conductive processes of energy transfer (Conway and Rasmussen, 2000; Nicholson and Benn, 2012; Petersen et al., 2022). These processes have been investigated in model studies of energy fluxes through the debris cover that allow for ventilation through the debris (Evatt

et al., 2015), stratification of moisture content and associated phase changes within the debris layer (Collier et al., 2014; Evatt et al., 2015; Giese et al., 2020) or stratification of thermal properties (Laha et al., 2022; Petersen et al., 2022). Multi-layered applications of the thermal diffusion representation of the debris layer have been presented for specific purposes in recent literature. For example, Laha et al. (2022) focus on developing an optimal way to estimate sub-debris melt rates directly from minimal debris temperature observations. For this, they perform multiple rather than single regression analysis to account for (i) unknown depth variation in thermal diffusivity in a two-layer model and (ii) non-conductive heat sources/sinks. They compare the derived heat transfer using the method of Conway and Rasmussen (2000), to their newly introduced Bayesian inversion method of determining debris thermal properties, for both homogenous and prescribed two-layer debris properties, limiting their analysis to three temperature measurements within the debris, and avoiding measurements from the near surface where non-conductive processes are expected to contribute a larger portion of energy flux. For the homogenous debris case they highlight the importance of equal vertical spacings between thermistors to reduce truncation errors, and show that if unequal spacing cannot be avoided, the Bayesian method outperforms that of Conway and Rasmussen (2000). As expected, for the two layer debris case they demonstrate that the model versions accommodating this structure outperform model versions forced to solve for a single layer. Petersen et al. (2022) focus their analysis on identifying the presence of non-conductive heat transfer processes. For this, they also included a term for depth varying thermal diffusivity into the heat conduction equation and perform multiple linear regression to solve for thermal diffusivity and its variation with depth in natural debris cover, identifying non-conductive processes as the residual from a comparison of the observed and modelled time dependent temperature evolution. They find non-negligible heat transfer related air motion and latent heat fluxes within the debris on Kennicott Glacier. Nevertheless, the method of Conway and Rasmussen (2000) remains the key tool to derive debris thermal properties for subsequent use in generalised surface energy balance models. The approach is to identify layers and periods of debris temperature profile data that can be identified as being 'well-behaved' approximations of a conductive system. Then the apparent thermal diffusivity can be determined for this well-behaved section of the observations, and from this, the effective thermal conductivity of the rocks can be calculated by making some educated assumptions of the porosity and what the pores are filled with. For example, in an ideal case, one can determine effective thermal conductivity from a dry portion of the debris with consistent grain size and minimal non-conductive processes. When used in a surface energy balance model, the derived effective thermal conductivity for dry debris can be modified by introducing the effects of pore water phase changes by prescribing or simulating likely debris saturation levels to simulate the complete debris cover (Collier et al., 2014; Giese et al., 2020). The majority of debris effective thermal conductivity values used within surface energy balance models in the published literature use this Conway and Rasmussen (2000) approach, yet little effort has yet been made to critically assess if the sensor deployment and analysis strategy used is optimal or comparable across studies. The limited number of field datasets used to provide generalized values for the effective thermal conductivity of unmeasured glacier sites have been produced following Conway and Rasmussen (2000), without critical consideration of the impact of the specifics of how the method is applied. Therefore, a deeper exploration of the limitations to interpreting values derived by this method is warranted, in particular to better understand the meaning of comparison of derived thermal conductivity values between sites at regional and global scales (e.g. Rowan et al., 2021; Miles et al., 2022). For example, the measurement parameters for temporal or spatial sampling

intervals, thermistor spacings, and debris depths used in the application of the standard method presented by Conway and Rasmussen (2000) are selected ad hoc in different studies and differ from measurement site to measurement site (e.g. Juen et al., 2013; Chand and Kayastha, 2018; Rowan et al., 2021), and uncertainty estimates associated with this are not addressed in the published literature. As a consequence, baseline literature values that are subject to onward use in surface energy balance modelling may be differently influenced by sensor, installation and numerical truncation errors.

2 Aim of this study

This study explores the effect of the chosen temporal and vertical spatial temperature sampling interval and other systematic measurement errors originating in the measurement setup on the derived thermal diffusivity values. By doing so, the roles of these different error sources can be quantified and a more critical reassessment of the extent to which differences in published effective thermal conductivity values reflect real world differences in debris properties or instrumental and analytical choices becomes possible. To explore the capabilities and limitations of deriving apparent thermal diffusivity following Conway and Rasmussen (2000) we apply this method to artificially generated data with a known value of thermal diffusivity, which allows us to individually quantify systematic and statistical errors by error source. We additionally present an online tool to allow interactive analysis of these combined errors for a given dataset and a best practice guideline on how to minimize the systematic errors of using this method. The study was first presented at the EGU General Assembly 2021 (Beck and Nicholson, 2021).

3 Methods

3.1 Artificial data for benchmarking derived thermal diffusivity

To test the method of Conway and Rasmussen (2000) for different scenarios, we generate artificial measurement data for debris cover thicknesses of 30, 100 and 200 cm and thermal diffusivity values of $5 \cdot 10^{-7} m^2 s^{-1}$, and $10 \cdot 10^{-7} m^2 s^{-1}$, to represent a range of values obtained from previous field studies from glaciers across the globe (Laha et al., 2022). To generate data for a perfectly conductive system, we force the heat equation by five surface temperature time-series and a boundary condition for the debris ice interface at 0°C. The five different scenarios of 10 days of diurnal surface temperature cycles are; a pure sinusoidal daily cycle, a skewed cycle, and three different types of measurement data from previous measurements (Fig. 2). The first two days of temperature forcing data are used to initialize the model, and the different depths of the debris layer are represented by varying the number of vertical grid points maintaining equidistant spacing.

We use the method by Crank and Nicolson (1947) to solve the heat conduction equation for this set of given constraints. This implicit finite difference method is convergent second-order in time and numerically stable. The method is based on the trapezoidal rule and is a combination of the Euler forward and backward methods in time. For the thermal heat equation, it results in the following equations:

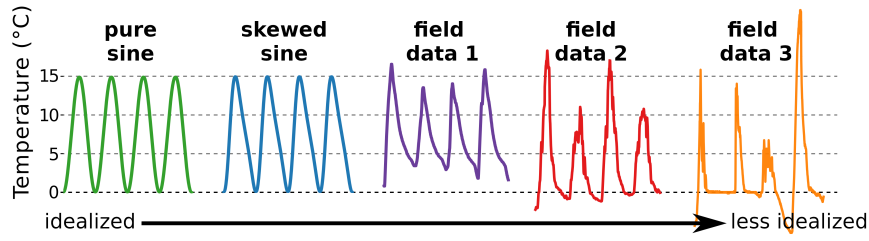


Figure 2. Characteristics of the surface temperature forcing for the artificial data generation consisting of two analytical sine curves and three experimental temperature measurements within the debris layer. The sine curves have a average temperature of 7.5°C and the same amplitude. Surface forcing from field data is derived from the upper most thermistor which lies 1-5cm below the surface, as indicated in brackets. Field data 1 and 3 was recorded at Lirung glacier (Nepal) during September 2013 (5cm below surface) and April 2014 (1cm below surface) respectively and was by provided by Chand and Kayastha (2018). Field data 2 was recorded at Vernagtferner (Austria) during June 2010 (4cm below surface) and was provided by Juen et al. (2013). The color scheme of these forcings is used in subsequent figures.

$$\frac{T_i^{n+1} - T_i^n}{\Delta t} = \frac{\kappa}{\Delta x^2} (T_{i+1}^{n+1} - 2T_i^{n+1} + T_{i-1}^{n+1}) \quad (\text{forward Euler}) \quad (3)$$

$$\frac{T_i^{n+1} - T_i^n}{\Delta t} = \frac{\kappa}{\Delta x^2} (T_{i+1}^n - 2T_i^n + T_{i-1}^n) \quad (\text{backward Euler}) \quad (4)$$

Combining these results in the Crank-Nicolson scheme:

$$135 \quad \frac{T_i^{n+1} - T_i^n}{\Delta t} = \frac{\kappa}{2\Delta x^2} \left((T_{i+1}^{n+1} - 2T_i^{n+1} + T_{i-1}^{n+1}) + (T_{i+1}^n - 2T_i^n + T_{i-1}^n) \right) \quad (5)$$

Because of the implicit nature of the Crank-Nicolson scheme, an algebraic equation or linearizing the equation is necessary to solve the next time step. In the case of our model, we can use the boundary conditions $T(x=0, t) = f(t)$ and $T(x=D, t) = 0$. Here $f(t)$ represents the arbitrary temperature forcing function (Fig. 2). Although the method is unconditionally numerically stable for the heat equation (Thomas, 2013), unwanted spurious oscillations can occur if the time steps are too long or the spatial resolution is too small. To avoid this, von Neumann stability conditions must be fulfilled (Charney et al., 1950):

$$140 \quad \kappa \frac{dt}{dx^2} \leq \frac{1}{2} \quad (6)$$

The artificial data was generated at five minute and two centimeter resolution, in order to meet this stability criteria for both tested values of thermal diffusivity. The resulting test data (e.g. Fig. 3) provides an ideal reference from which temperatures can be sampled in space and time to replicate field measurements, in order to examine the behaviour of the established methods of extracting thermal conductivity values from real-world datasets.

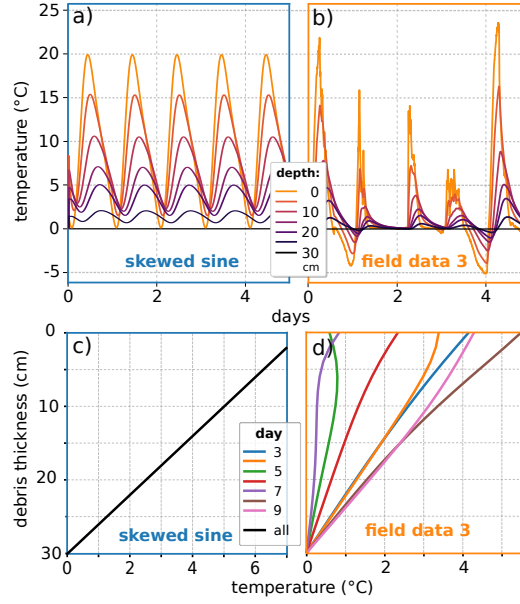


Figure 3. Artificially generated debris layer temperature timeseries data for the skewed sine forcing (a) and the field data 3 forcing (b) for a 30 cm debris layer and thermal diffusivity of $5 \cdot 10^{-7} m^2 s^{-1}$ using Crank-Nicolson scheme. (c and d) Daily averaged debris layer temperature profile for the boundary conditions in the upper panels, show that the often-used steady-state assumption (Evatt et al., 2015) of the daily mean debris layer temperature, shown by a linear temperature gradient, is only fulfilled for periodic daily temperature forcings.

3.2 Simulations performed

3.2.1 Quantifying truncation errors in space and time

The first analysis step is to calculate the truncation error due to the central difference scheme for different temporal and spatial sampling intervals. In theory, the numerical solution should be equal to the analytical solution for infinitesimally small spatial and temporal sampling intervals. Truncation errors are expected to scale with the temporal and spatial increment of the analysis with respect to the diurnal forcing cycle (Laha et al., 2022). Higher-order approximations would reduce the truncation error, but errors due to measurement uncertainties would dominate, as described by Zhang and Osterkamp (1995).

$$\lim_{\Delta t \rightarrow 0} \frac{T_{t+1} - T_{t-1}}{2\Delta t} = \dot{T} \quad \& \quad \lim_{\Delta x \rightarrow 0} \frac{T_{x+1} - T_x + T_{x-1}}{(\Delta x)^2} = T'' \quad (7)$$

For $\Delta x, \Delta t = 0$ the equations are not solvable.

We calculate the relative error as:

$$\text{Relative error} = \frac{\kappa_{\text{True}} - \kappa_{\text{Estimated}}}{\kappa_{\text{True}}} \quad (8)$$

Here, positive relative error values correspond to an underestimation of thermal diffusivity values.

For the temporal resampling, we compare sampling by skipping and sampling by averaging (Fig 4). When skipping, we only select every n -th value and omit the rest. The alternative resampling is to average over n values, which reduces gradients and therefore the analysis results are expected to underestimate compared to reality. Nevertheless we include this approach as some published field data collection campaigns are based on measurements of averages instead of sampled temperatures (e.g. Rowan et al., 2021). For the spatial resampling we skip data points in space.

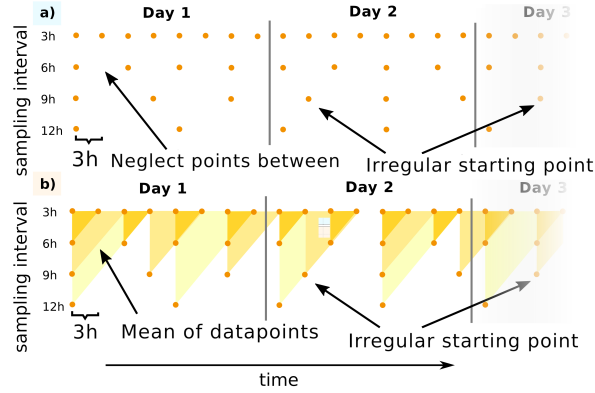


Figure 4. Comparing two different temporal resampling methods by displaying the temporal grid for different sampling intervals. We compare the method by skipping every n -th gridpoint (a - blue background) or by averaging over n gridpoints (b - orange background).

3.2.2 Quantifying sensor and installation errors

Thermistors buried in supraglacial debris to record the temperature profiles over time, have varying, manufacture stipulated sensor precision. To simulate the effect of temperature measurement precision, we discretize the temperature data to correspond with the measurement uncertainty of 0.1 to 0.4 °C, which is representative of the precision of thermistors typically used in the field.

Vertical measurements of temperatures through the debris layer must be accompanied by a known depth of measurement within the layer. However, these can be challenging to measure with a high degree of accuracy in the field, and additionally, the thermistors may migrate within the debris layer if there is any motion of the debris, which could alter their relative distance over time. To simulate the vertical displacement of a thermistor we set the temperature uncertainty back to zero and add a gaussian uncertainty on the vertical thermistor position of 0.25 and 0.5 centimeters. In reality, if thermistors move within the debris due to settling or debris migration, the positional inaccuracy could be even be larger, but this would likely be discernible from evidence of debris movement or identified when the thermistors were removed from the debris layer, allowing affected data to be excluded from further analysis.

4 Results

First the artificial data is used without any added sensor or installation uncertainty to examine the behaviour of truncation errors. Subsequently the errors associated with the sensor and installation uncertainty are presented.

4.1 Error due to temporal truncation

180 The relative temporal truncation error has a monotonous increasing trend for an increasing sampling time for the skipping method (Fig. 5a,b), with the exact form being dependent on the forcing used; for example, the errors for the sine curve are comparable throughout the debris layer for different sampling methods, while the noisier field data forcing produces errors that differ with depth in the debris.

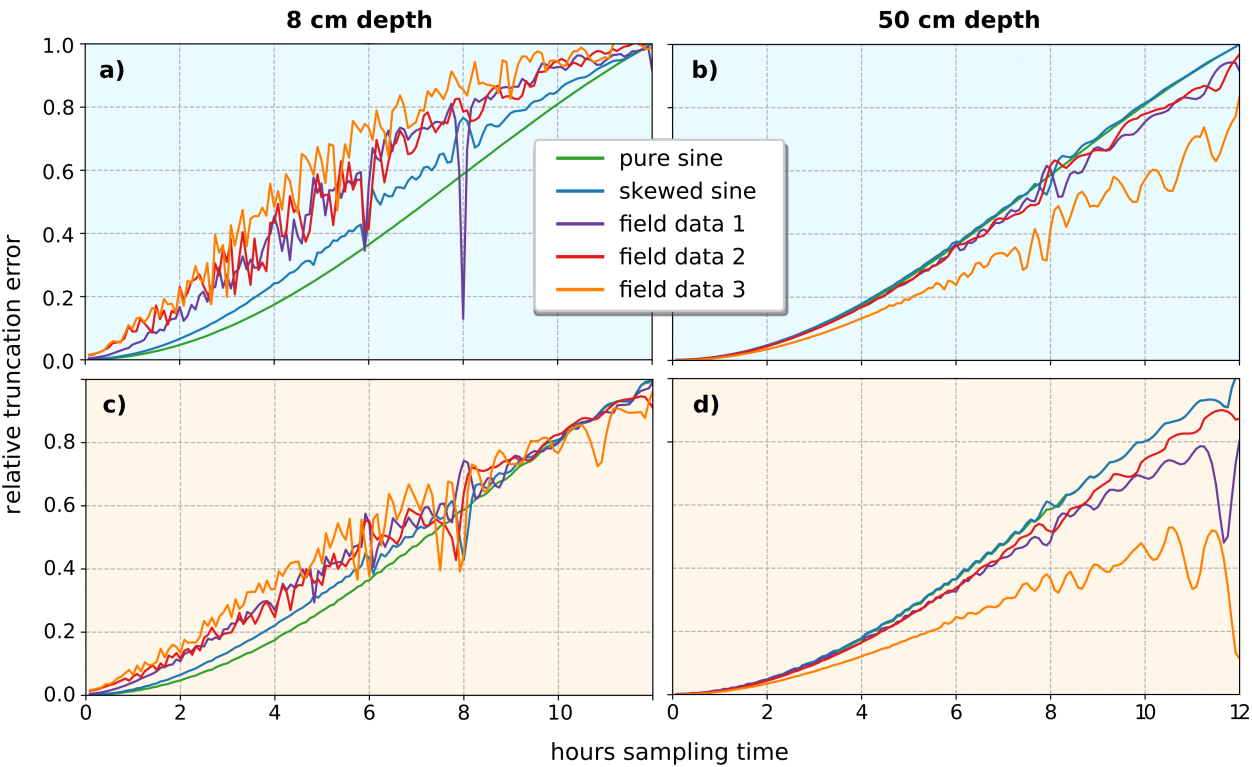


Figure 5. Relative temporal truncation error of thermal diffusivity estimation by sampling interval: Comparison of different temperature forcing for skipping (a,b - blue background) and averaging (c,d - orange background) re-sampling methods for two different depths in the 100 cm debris layer.

At shallow depths, the less sinusoidal the temperature forcing is, the larger the error at small sampling intervals (Fig. 5a, c).
185 When data is resampled by averaging, the temporal error is less extreme but shows similar behavior to the skipping method (Fig. 5c). At greater depths in the debris, the noisy surface diurnal signals tend to be more similar to those of the sinusoidal

surface forcing (Fig. 5b, d). Consistently positive relative truncation errors due to the temporal sampling interval systematically underestimate values of thermal diffusivity and therefore can be expected to systematically underestimate glacier melt. Therefore from a truncation perspective, a minimum temporal resolution is desirable, and selecting days with surface temperature forcing that is closer to sinusoidal will decrease errors at shallow depths.

4.2 Error due to spatial truncation

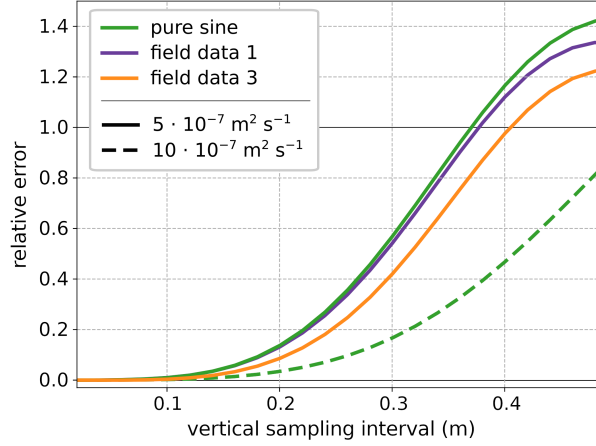


Figure 6. Comparison of the spatial truncation error for different thermal diffusivity values and forcing types over vertical sampling ranges up to 0.5m.

Spatial truncation error values (Fig. 6) remain quasi-constant for low Δx , up to when the centered differencing scheme spans more than 0.2m, and thereafter increases rapidly with increasing Δx . The spatial truncation error is similar for the different surface temperature forcings, and in contrast to the temporal truncation error does not vary markedly with debris depth. Instead the value of thermal diffusivity imposes a strong influence, with higher thermal diffusivity cases having smaller errors. Given that the diffusivity is the target of sensor installations, this parameter cannot be known in advance as the results suggest that Δx of up to 0.1 meters is desirable. Again the consistently positive error values mean that the spatial source of truncation error also has the tendency to systematically underestimate glacier melt, and increasingly so with more widely spaced temperature measurements.

4.3 Error due to thermistor precision

To examine the role of temperature sensor precision, we focus on the range of sensor spacings that are not affected by the truncation error, i.e. for Δx up to 0.14m (Fig. 7). Because we added temperature uncertainty, it now makes a difference how we sample the thermistor spacings. One can either start at the top - so from the surface layer - and increase the Δx from there, or the middle of the debris layer and selects Δx symmetrically, or start at the debris-ice interface and go up from there with increasing measurement uncertainty. For small values of Δx the relative error spikes and exponentially decreases for larger

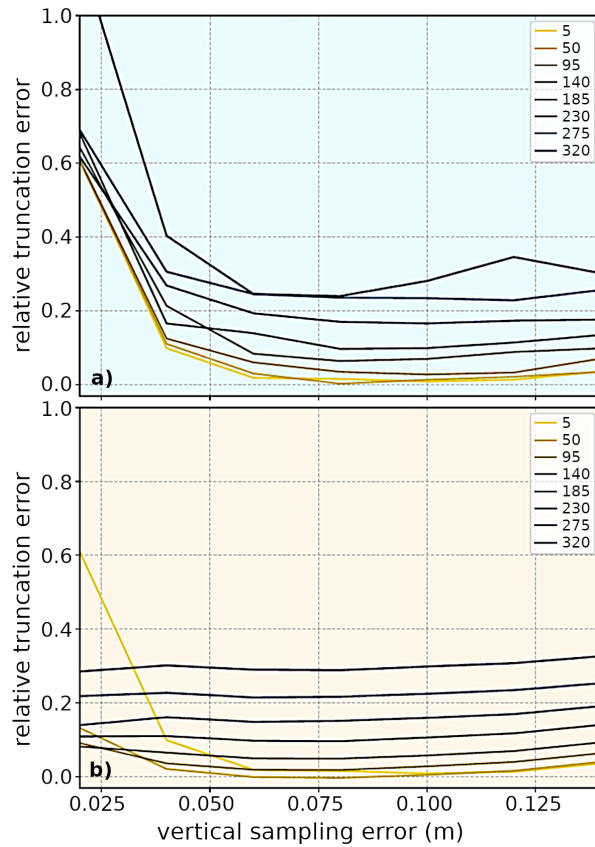


Figure 7. Relative error of estimated thermal diffusivity value due to thermistor temperature discretisation of 0.4°C while comparing the (a) skipping and (b) averaging method. Sampled from the surface layer downward.

values of Δx . The averaging method produces different but similar results. We see that this error is less pronounced for smaller temperature discretizations, representing greater thermistor precision. Values of Δx between the dominant spatial truncation error and the error due to the uncertainty are desirable, so between 5 and 15 centimeters. This error would systematically underestimate glacier melt.

210 4.4 Error due to uncertain sensor depth in debris

As demonstrated in subsection 4.2, the relative error increases with increasing thermistor spacing due to the smaller gradients, but we additionally want to understand the depth dependence of constant vertical sampling intervals (Fig. 8).

For a Δx of two centimeters, only measurements with a maximum thermistor uncertainty of 0.01 °C would produce correct values, and then only for the first 20 centimeters of debris. Switching to an Δx of 6 centimeters, the relative error decreases for
 215 all curves. Still, the thermistors used in most field experiments, which have reported precision ranging from 0.1 to 0.4 °C would not produce correct values. When increasing the sampling time to beyond 60 minutes, results improve for the layers close to

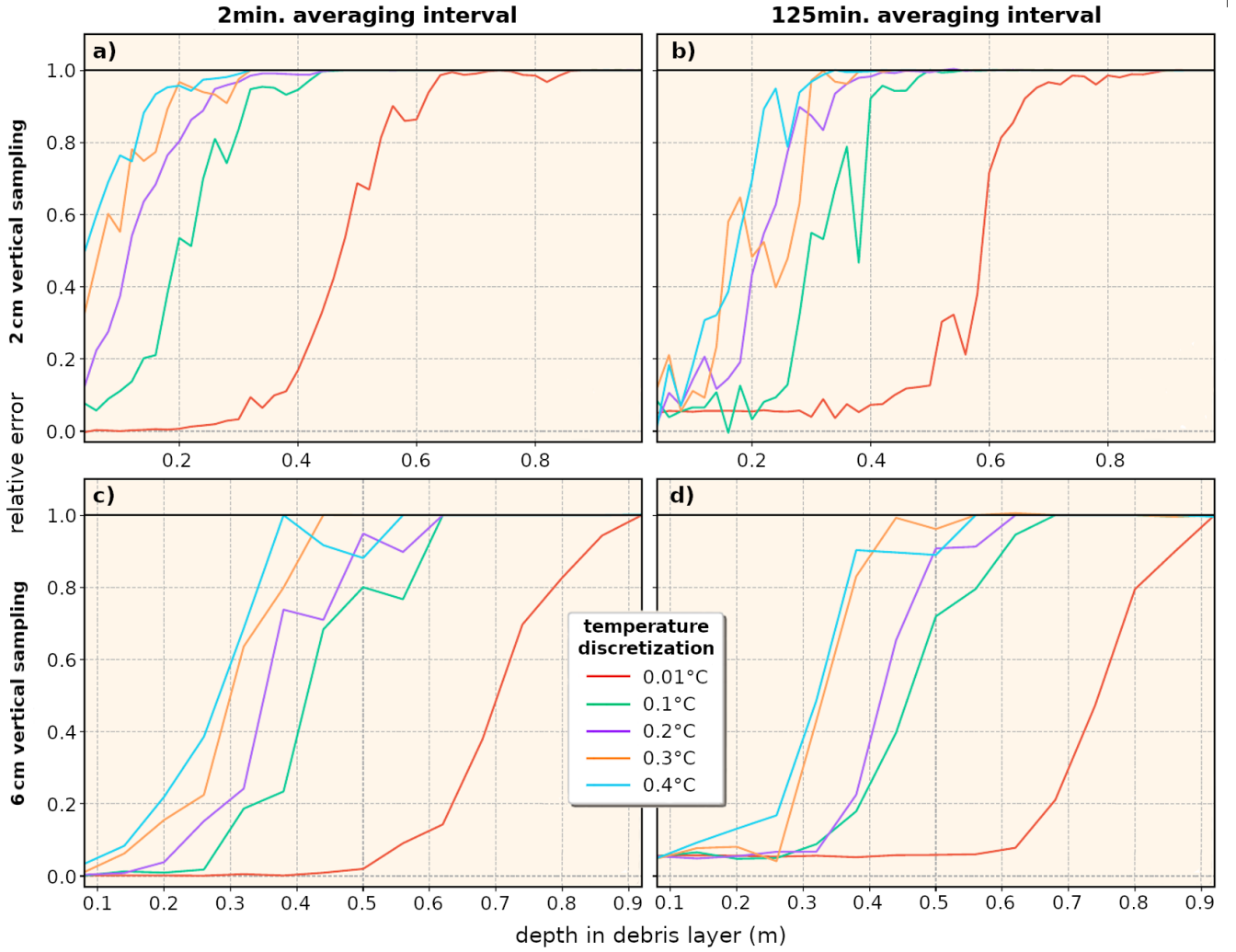


Figure 8. Relative error of estimated thermal diffusivity value due to thermistor discretization by depth in the debris up to 0.9 m, with the different color lines corresponding to different values of temperature uncertainty/sensor precision.

the surface before the temporal truncation error becomes relevant. For higher sampling intervals, the averaging method here performs even better. This shows the importance of deploying thermistors with the highest accuracy and precision possible, even when using larger spatial sampling intervals. At depths beyond 0.5m it becomes difficult to obtain correct values even with high-resolution thermistors, at least for the forcing conditions trialled in our analysis.

4.5 Error due to vertical thermistor position variability

Conway and Rasmussen (2000) report that a vertical error of 0.5 cm would result in a marginal temperature difference of 0.1 K and 0.02 K for their measurement setups. This is then interpreted by them and others (e.g. Nicholson and Benn, 2012) that a vertical thermistor displacement would not affect the results as long as this value does not change in time.

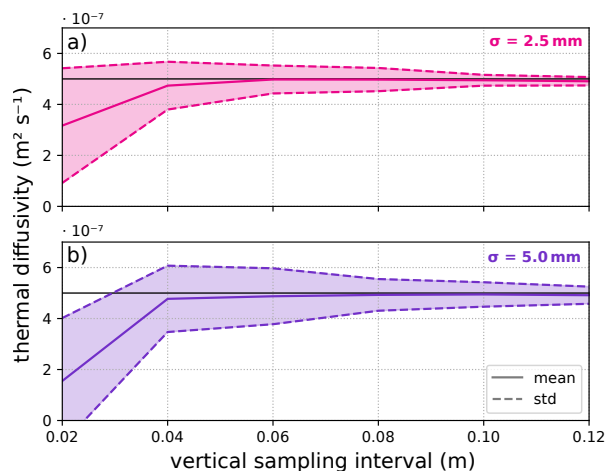


Figure 9. Illustrating the influence of thermistor displacement on calculated thermal diffusivity, by randomly displacing locations by a normal distribution with standard deviation of (a) 0.25 cm and (b) 0.5 cm over a range of vertical spacing intervals. The true/target thermal diffusivity is shown by the horizontal black line, showing that for small temperature sampling intervals sensor displacement results in large inaccuracies in calculated thermal diffusivity.

225 This error source is the only one in the course of this study that has the potential to increase thermal diffusivity values shown in Fig. 9 by the spread of values of thermal diffusivity larger than the black reference value line. For sensors installed with a Δx of two centimeters, the resultant error on calculated values of effective thermal diffusivity is so large that the data would become unusable. With increasing Δx , the relative error decreases until a distance is reached where the spatial truncation error becomes relevant again (see section 4.2).

230 5 Discussion

Conway and Rasmussen (2000) provide a simple and easy to apply method to estimate thermal diffusivity values from a vertical array of thermistors in the debris layer, but our analysis demonstrates that the calculated diffusivity values are sensitive to instrumental set up and analysis choices. Although this method has become the standard method for determining effective thermal conductivity to be used in surface energy balance models of sub-debris ice ablation (e.g. Nicholson and Benn, 2006; Juen et al., 2013; Nicholson and Benn, 2012; Rounce et al., 2015; Chand and Kayastha, 2018; Rowan et al., 2021), it is regularly used without considering these error sources, making it difficult to robustly compare published values derived using

this method. To address this, we provide an open source tool where researchers can investigate the combined opportunities and limitations of applying the method by Conway and Rasmussen (2000) to glaciology and beyond and we hope this facilitates more consistent and rigorous experimental design in future field measurements determining debris thermal properties, and also facilitates reanalysis of published values being compared across regions. The tool, available at <https://github.com/calvinbeck/TC-DTD> is coded in Python and includes two user friendly Jupyter Notebooks (Kluyver et al., 2016) to allow users to simulate their own artificial data and repeat all our analyses presented here with their own artificial or field datasets.

In previously published values, most apparent thermal diffusivity derived using the method of Conway and Rasmussen (2000) are below $10 \cdot 10^{-7} m^2 s^{-1}$, typically ranging from 1 to 30 with some outlier values exceeding $100 \cdot 10^{-7} m^2 s^{-1}$ (see Table 2 in Laha et al., 2023). The errors that our analysis reveals are often comparable to this range of published values, highlighting how relevant these considerations are. Of the error sources investigated here, all truncation errors, and errors due to measurement uncertainties, systematically underestimate thermal diffusivity values. Too large temporal or spatial sampling intervals both result in non-negligible non-linear truncation errors. Near-surface measurements are especially problematic because the diurnal temperature cycle is most non-sinusoidal within the debris layer and therefore produces larger temporal truncation errors. Conditions that more closely approximate sinusoidal conditions are associated with clear sky stable atmospheric conditions, and surface noise introduced by weather is progressively smoothed out at greater depth in the debris. Even though a Δt or $\Delta x \rightarrow 0$ would produce a minimal truncation error, too small sampling intervals also can produce erroneous results because for a $\Delta t \rightarrow 0$, the linear regressions coefficient of determination decreases strongly. In practice, this is not a problem since short temporal sampling intervals can always be resampled afterwards. A more significant problem is if thermistors are positioned too close to each other, especially if the profile is comprised of only a few thermistors, making it impossible to spatially resample the temperature data. With increasing depth, the thermistors in the debris layer have to be positioned further apart otherwise, the thermistor measurement uncertainty dominates the measurement. Therefore, at greater depths in the debris layer, it is not wise to perform measurements with low precision instruments ≤ 0.01 K.

The only error source investigated here that has the potential to overestimate the thermal diffusivity value is that due to vertical displacement of the thermistors within a mobile debris cover. This can happen due to debris settling after sensor installation or if the thermistor profiles are installed on a slope, that is subject to gradual gravitational sliding or reworking. In contrast to the derivation by Conway and Rasmussen (2000), who showed that a constant error in the thermistor was not important to the analysis, we find that the calculated value of thermal diffusivity does depend on the thermistor positions relative to each other being correctly known and sustained over the measurement period.

In the best practice guidelines (Appendix A) we address all sources of error discussed in this paper and are the basis for producing more reliable measurement data and therefore the most robust values of apparent thermal diffusivity following the method of Conway and Rasmussen (2000). They can be used to develop optimal implementation strategy for future field studies that wish to deploy these methods of analysing representative thermal conductivity of natural debris layers. Our recommendations differ from those of Laha et al. (2022), as the purpose is different. While Laha et al. (2022), sought to determine the optimal method to determine sub-debris ablation rates directly from temperature sensors, we seek to understand the best way to determine a representative apparent thermal diffusivity, from which effective thermal conductivity suitable for onward

use in generalised surface energy balance models can be derived. For their purpose, they propose to "set the sensor spacing to be $1/5^{\text{th}}$ of the debris thickness at the location", however the non-linear nature of the single error sources presented in this paper indicates that we cannot generalize such statements if the goal is parameter determination, rather than direct ablation determination. Furthermore, they stated "the top sensor should be placed approximately at the middle of the debris layer", as this captures the relevant flux being delivered to the underlying ice. Our analysis indicates that while it is true that thermistors too close to the surface produce large truncation errors, the same is valid for too deep thermistors as the temperature gradient is too small relative to the thermistor precision.

In addition to the errors related to measurement set up and analysis procedure investigated in this study, non-conductive processes within the debris layer (e.g. rain, phase changes) would distort the results (Conway and Rasmussen, 2000; Nicholson and Benn, 2012; Petersen et al., 2022). At present it is not always clear in the published literature that the derived thermal diffusivities and associated thermal conductivity values were derived from the optimal conditions sampled within the dataset. The suitability of the sampled debris temperature profiles for determining debris thermal parameters must be carefully evaluated on a case-by-case basis using meteorological data and closely evaluating the measurements and their gradient functions (Petersen et al., 2022) in order to Apparent thermal diffusivities calculated from conditions approximating conductive ones can then be used to derive thermal conductivity with some assumptions of the ambient grain size, porosity and related pore space fluid. These base values of thermal conductivity can be modified in implementation within a surface energy balance model to account for changes in the pore fluid type to allow simulation of varying wet/dry debris conditions (Collier et al., 2014; Giese et al., 2020). Reanalysing previously published vertical temperature profiles using the methods of Petersen et al. (2022) and/or Laha et al. (2022) might yield more robust and representative global values by providing respectively a more rigorous assessment, or inclusion, of non-conductive processes or multilayered thermal properties within the sampled debris layers.

6 Conclusion

Surface energy balance models of sub-debris ice ablation typically solve the energy balance at the surface of the debris, using a conductive ground heat flux representing the energy transfer through the debris to the ice. Sub-debris ice ablation is then calculated from the resultant heat flux at the debris ice interface. In order to apply such a model one of the required known properties that is difficult to determine is the effective thermal conductivity of the debris cover. This parameter is commonly determined from field measurements of vertical profiles of debris temperatures and heat diffusion theory, but its application is non-standardised across different studies, impeding assessments of the robustness or comparability of reported values of this parameter in the published literature.

Our analysis highlights that it is challenging to interpret derived thermal properties if the sensor and analysis system is not reported and accounted for, leaving considerable room for error, especially since the datasets often lack relevant meta- and meteorological data. We encourage more rigorous reporting of published measurement uncertainty in order to facilitate cross-comparison of reported results. To facilitate this, we provide a tool for exploratory data analysis that can be used to determine

optimal data recording strategies for field observations or to reanalyse datasets consistently over space or time in order to
305 support regional intercomparison of derived values.

While recent publications highlight limitations of the simplest deployment of the heat diffusion equation in natural debris layers due to the role of non-conductive processes and internal debris stratification, our analysis and best practice guidelines show the sampling strategies that will yield the best results, provided that the temperatures underpinning the analyses demonstrably sample conditions that closely approximate a homogenous conductive system.

310 *Code availability.* Publicly available under: <https://github.com/calvinbeck/TC-DTD>

Author contributions. This publication is based on the MSc thesis of CB, supervised by LN. LN conceived the study, CB performed all analysis, developed the online tool, produced the figures and led the preparation of the manuscript. Both CB and LN worked to finalise the manuscript for publication.

Competing interests. The authors declare that they have no conflict of interest.

315 *Acknowledgements.* Field datasets used for temperature forcing in this analysis (Fig. 2) were provided by Mohan Chand, Rijan Kayastha, Martin Juen and Christoph Mayer. In the course of the Masters thesis analysis further forcing data was provided by members of the IACS working group on Debris Covered Glaciers (<https://cryosphericsscience.org/activities/wgdebris/>).

Appendix A: Best practice guidelines

Our analysis leads us to the following best practice guidelines to help other researchers to get as much as possible out of their
320 measurements.

Thermistor precision:

As small as possible, but not larger than 0.1 K.

Debris layer thickness:

To determine a representative thermal diffusivity from which robust, generally applicable, thermal conductivity values can be derived, sampling a minimum of 40 cm but ideally deeper (e.g. 100 cm) debris thickness is advised. The maximum depth that can be meaningfully sampled is limited by the thermistor precision and temperature gradients in the debris layer, which can be simulated beforehand using the provided tool.

Number of thermistors:

The method requires at least three thermistors, but more thermistors make it possible to calculate diffusivity values for different depths and therefore makes it possible to identify non-conductive processes or other inconsistencies within the debris layer. With only three temperature sensors it is difficult to assess if the sampled debris meets the requirement of closely approximating a conductive system. A second redundant set of thermistors can also be helpful to rule out measurement errors.

Thermistor installaton:

Choose a site that is not expected to be subject to gravitational reworking or sliding of the debris, and where lateral heat fluxes are expected to be minimal. Place thermistors at equal vertical intervals of 8 to 20 cm. Even though the uppermost layer often does not produce ideal results, it can be helpful to place a thermistor at the debris-surface interface still because, this way, the debris layer can subsequently be simulated. Depending on the depth, the thermal diffusivity, and temperature gradient of the debris layer, the method produces more significant errors with a greater depth limiting the depth where it makes sense to place thermistors. The sweet spot can be determined by simulating the debris layer of interest beforehand with model parameters from previous measurements or other estimations.

Thermistor recovery:

Thermistors have to be carefully extracted, and their vertical positions recorded, at the end of the measurement period to make sure the thermistors haven't moved in the debris while deployed. In case the thermistors moved, it might be necessary to discard the dataset. Therefore mounting thermistors to a thermally insulated rod or set of rods so that their positions are fixed is a valuable approach to eliminate this potential error source.

Temporal sampling interval:

Sample with a temporal resolution as short as possible and then average over a 5 minute period. Over such a short period, the temperature is assumed to be nearly constant and therefore not to reduce gradients. By averaging the temperature over a short interval, discretization is reduced.

Measurement duration and conditions:

It depends on the scientific objective and seasonality, but at least a week of suitable stable meteorological conditions are needed. Therefore, if one has unlucky conditions, a measurement duration of several months could be necessary. A shorter period of predominantly sinusoidal surface temperature forcing and evidence that non-conductive processes are minimal is the best way to obtain robust values, so avoiding periods of precipitation, seasonal change and phase change is advised.

330 References

- Adhikary, S., Seko, K., Nakawo, M., Ageta, Y., and Miyazaki, N.: Effect of surface dust on snow melt, *Bulletin of glacier research*, 15, 85–92, 1997.
- Anderson, R. S., Anderson, L. S., Armstrong, W. H., Rossi, M. W., and Crump, S. E.: Glaciation of alpine valleys: The glacier–debris-covered glacier–rock glacier continuum, *Geomorphology*, 311, 127–142, <https://doi.org/10.1016/j.geomorph.2018.03.015>, 2018.
- 335 Beck, C. and Nicholson, L.: Assessing the time-step dependency of calculating supraglacial debris thermal diffusivity from vertical temperature profiles, in: EGU General Assembly Conference Abstracts, pp. EGU21–13 402, <https://doi.org/10.5194/egusphere-egu21-13402>, 2021.
- Benn, D., Bolch, T., Hands, K., Gulley, J., Luckman, A., Nicholson, L., Quincey, D., Thompson, S., Toumi, R., and Wiseman, S.: Response of debris-covered glaciers in the Mount Everest region to recent warming, and implications for outburst flood hazards, *Earth-Science*
- 340 *Reviews*, 114, 156–174, <https://doi.org/https://doi.org/10.1016/j.earscirev.2012.03.008>, 2012.
- Bhambri, R., Bolch, T., Chaujar, R. K., and Kulshreshtha, S. C.: Glacier changes in the Garhwal Himalaya, India, from 1968 to 2006 based on remote sensing, *Journal of Glaciology*, 57, 543–556, <https://doi.org/10.3189/002214311796905604>, 2011.
- Bolch, T., Kulkarni, A., Kääb, A., Huggel, C., Paul, F., Cogley, J. G., Frey, H., Kargel, J. S., Fujita, K., and Scheel, M.: The state and fate of Himalayan glaciers, *Science*, 336, 310–314, <https://doi.org/10.1126/science.1215828>, 2012.
- 345 Brock, B. W., Mihalcea, C., Kirkbride, M. P., Diolaiuti, G., Cutler, M. E., and Smiraglia, C.: Meteorology and surface energy fluxes in the 2005–2007 ablation seasons at the Miage debris-covered glacier, Mont Blanc Massif, Italian Alps, *Journal of Geophysical Research: Atmospheres*, 115, <https://doi.org/10.1029/2009JD013224>, 2010.
- Cannon, J. R.: *The one-dimensional heat equation*, Cambridge University Press, 1984.
- Chand, M. B. and Kayastha, R. B.: Study of thermal properties of supraglacial debris and degree-day factors on Lirung Glacier, Nepal, *SCAR*, 10, 357–368, <https://doi.org/10.3724/SP.J.1226.2018.00357>, 2018.
- 350 Charney, J. G., Fjörtoft, R., and Von Neumann, J.: Numerical integration of the barotropic vorticity equation, in: *The Atmosphere — A Challenge*, pp. 267–284, Springer, https://doi.org/10.1007/978-1-944970-35-2_15, 1950.
- Collier, E., Nicholson, L., Brock, B., Maussion, F., Essery, R., and Bush, A.: Representing moisture fluxes and phase changes in glacier debris cover using a reservoir approach, *The Cryosphere*, 8, 1429–1444, <https://doi.org/10.5194/tc-8-1429-2014>, 2014.
- 355 Conway, H. and Rasmussen, L. A.: *Summer temperature profiles within supraglacial debris on Khumbu Glacier, Nepal*, IAHS Publications, 264, 89–98, 2000.
- Crank, J. and Nicolson, P.: A practical method for numerical evaluation of solutions of partial differential equations of the heat-conduction type, *Mathematical Proceedings of the Cambridge Philosophical Society*, 43, 50–67, <https://doi.org/10.1017/S0305004100023197>, 1947.
- Deline, P. and Orombelli, G.: Glacier fluctuations in the western Alps during the Neoglacial, as indicated by the Miage morainic amphitheatre
- 360 (Mont Blanc massif, Italy), *Boreas*, 34, 456–467, <https://doi.org/10.1111/j.1502-3885.2005.tb01444.x>, 2005.
- Evatt, G. W., Abrahams, I. D., Heil, M., Mayer, C., Kingslake, J., Mitchell, S. L., Fowler, A. C., and Clark, C. D.: Glacial melt under a porous debris layer, *Journal of Glaciology*, 61, 825–836, <https://doi.org/10.3189/2015JoG14J235>, 2015.
- Fourier, J.-B.-J.: *The analytical theory of heat*, Courier Corporation, 1955.
- Fyffe, C. L., Reid, T. D., Brock, B. W., Kirkbride, M. P., Diolaiuti, G., Smiraglia, C., and Diotri, F.: A distributed energy-balance melt model
- 365 of an alpine debris-covered glacier, *Journal of Glaciology*, 60, 587–602, <https://doi.org/10.3189/2014JoG13J148>, 2014.

- Giese, A., Boone, A., Wagnon, P., and Hawley, R.: Incorporating moisture content in surface energy balance modeling of a debris-covered glacier, *The Cryosphere*, 14, 1555–1577, <https://doi.org/10.5194/tc-14-1555-2020>, 2020.
- Haidong, H., Yongjing, D., and Shiyin, L.: A simple model to estimate ice ablation under a thick debris layer, *Journal of Glaciology*, 52, 528–536, <https://doi.org/10.3189/172756506781828395>, 2006.
- 370 Herreid, S. and Pellicciotti, F.: The state of rock debris covering Earth's glaciers, *Nature Geoscience*, 13, 621–627, <https://doi.org/10.1038/s41561-020-0615-0>, 2020.
- Huo, D., Bishop, M. P., and Bush, A. B.: Understanding complex debris-covered glaciers: Concepts, issues, and research directions, *Frontiers in Earth Science*, 9, <https://doi.org/10.3389/feart.2021.652279>, 2021.
- Inoue, J. and Yoshida, M.: Ablation and Heat Exchange over the Khumbu Glacier Glaciological Expedition of Nepal, Contribution No. 65
 375 Project Report No. 4 on “Studies on Supraglacial Debris of the Khumbu Glacier”, *Journal of the Japanese Society of Snow and Ice*, 41, 26–33, https://doi.org/10.5331/seppyo.41.Special_26, 1980.
- Juen, M., Mayer, C., Lambrecht, A., Wirbel, A., and Kueppers, U.: Thermal properties of a supraglacial debris layer with respect to lithology and grain size, *Geografiska Annaler: Series A, Physical Geography*, 95, 197–209, <https://doi.org/10.1111/geoa.12011>, 2013.
- Kayastha, R. B., Takeuchi, Y., Nakawo, M., and Ageta, Y.: Practical prediction of ice melting beneath various thickness of debris cover on
 380 Khumbu Glacier, Nepal, using a positive degree-day factor, *IAHS Publications*, 7182, 2000.
- Kellerer-Pirklbauer, A., Lieb, G. K., Avian, M., and Gspurning, J.: The response of partially debris-covered valley glaciers to climate change: the example of the Pasterze Glacier (Austria) in the period 1964 to 2006, *Geografiska Annaler: Series A, Physical Geography*, 90, 269–285, <https://doi.org/10.1111/j.1468-0459.2008.00345.x>, 2008.
- Kirkbride, M. P. and Deline, P.: The formation of supraglacial debris covers by primary dispersal from transverse englacial debris bands,
 385 *Earth Surface Processes and Landforms*, 38, 1779–1792, <https://doi.org/10.1002/esp.3416>, 2013.
- Kirkbride, M. P. and Dugmore, A. J.: Glaciological response to distal tephra fallout from the 1947 eruption of Hekla, south Iceland, *Journal of Glaciology*, 49, 420–428, <https://doi.org/10.3189/172756503781830575>, 2003.
- Kluyver, T., Ragan-Kelley, B., Pérez, F., Granger, B. E., Bussonnier, M., Frederic, J., Kelley, K., Hamrick, J. B., Grout, J., Corlay, S., et al.: Jupyter Notebooks—a publishing format for reproducible computational workflows., *Elpub*, 2016, 87–90, <https://doi.org/10.3233/978-1-61499-649-1-87>, 2016.
 390
- Laha, S., Winter-Billington, A., Banerjee, A., Shankar, R., Nainwal, H. C., and Koppes, M.: Estimation of ice ablation on a debris-covered glacier from vertical debris-temperature profiles, *Journal of Glaciology*, 69, 1–12, <https://doi.org/10.1017/jog.2022.35>, 2022.
- Mattson, L. E.: Ablation on debris covered glaciers: an example from the Rakhiot Glacier, Punjab, Himalaya, *Intern. Assoc. Hydrol. Sci.*, 218, 289–296, 1993.
- 395 Mayer, C. and Licciulli, C.: The concept of steady state, cyclicity and debris unloading of debris-covered glaciers, *Frontiers in Earth Science*, 9, <https://doi.org/10.3389/feart.2021.710276>, 2021.
- Mihalcea, C., Mayer, C., Diolaiuti, G., Lambrecht, A., Smiraglia, C., and Tartari, G.: Ice ablation and meteorological conditions on the debris-covered area of Baltoro glacier, Karakoram, Pakistan, *Annals of Glaciology*, 43, 292–300, <https://doi.org/10.3189/172756406781812104>, 2006.
- 400 Miles, E. S., Steiner, J., Buri, P., Immerzeel, W., and Pellicciotti, F.: Controls on the relative melt rates of debris-covered glacier surfaces, *Environmental Research Letters*, 17, 064 004, <https://doi.org/10.1088/1748-9326/ac6966>, 2022.

- Minora, U., Senese, A., Bocchiola, D., Soncini, A., D'agata, C., Ambrosini, R., Mayer, C., Lambrecht, A., Vuillermoz, E., and Smiraglia, C.: A simple model to evaluate ice melt over the ablation area of glaciers in the Central Karakoram National Park, Pakistan, *Annals of Glaciology*, 56, 202–216, <https://doi.org/10.3189/2015AoG70A206>, 2015.
- 405 Nakawo, M. and Takahashi, S.: A simplified model for estimating glacier ablation under a debris layer, *IAHS Publications*, 138, 137–145, 1982.
- Nicholson, L. and Benn, D. I.: Calculating ice melt beneath a debris layer using meteorological data, *Journal of Glaciology*, 52, 463–470, <https://doi.org/10.3189/172756506781828584>, 2006.
- Nicholson, L. and Benn, D. I.: Properties of natural supraglacial debris in relation to modelling sub-debris ice ablation, *Earth Surface*
 410 *Processes and Landforms*, 38, 490–501, <https://doi.org/10.1002/esp.3299>, 2012.
- Nicholson, L., Wirbel, A., Mayer, C., and Lambrecht, A.: The challenge of non-stationary feedbacks in modeling the response of debris-covered glaciers to climate forcing, *Frontiers in Earth Science*, 9, <https://doi.org/10.3389/feart.2021.662695>, 2021.
- Østrem, G.: Ice melting under a thin layer of moraine, and the existence of ice cores in moraine ridges, *Geografiska Annaler*, 41, 228–230, <https://doi.org/10.1080/20014422.1959.11907953>, 1959.
- 415 Petersen, E., Hock, R., Fochesatto, G. J., and Anderson, L. S.: The Significance of Convection in Supraglacial Debris Revealed Through Novel Analysis of Thermistor Profiles, *Journal of Geophysical Research: Earth Surface*, 127, e2021JF006520, <https://doi.org/10.1029/2021JF006520>, 2022.
- Quincey, D. J. and Glasser, N. F.: Morphological and ice-dynamical changes on the Tasman Glacier, New Zealand, 1990–2007, *Global and Planetary Change*, 68, 185–197, <https://doi.org/10.1016/j.gloplacha.2009.05.003>, 2009.
- 420 Reid, T. D. and Brock, B. W.: An energy-balance model for debris-covered glaciers including heat conduction through the debris layer, *Journal of Glaciology*, 56, 903–916, <https://doi.org/10.3189/002214310794457218>, 2010.
- Reznichenko, N., Davies, T., Shulmeister, J., and McSaveney, M.: Effects of debris on ice-surface melting rates: an experimental study, *Journal of Glaciology*, 56, 384–394, <https://doi.org/10.3189/002214310792447725>, 2010.
- Rounce, D., Quincey, D., and McKinney, D.: Debris-covered glacier energy balance model for Imja–Lhotse Shar Glacier in the Everest
 425 region of Nepal, *The Cryosphere*, 9, 2295–2310, <https://doi.org/10.5194/tc-9-2295-2015>, 2015.
- Rounce, D. R., Hock, R., Maussion, F., Hugonnet, R., Kochtitzky, W., Huss, M., Berthier, E., Brinkerhoff, D., Compagno, L., Copland, L., et al.: Global glacier change in the 21st century: Every increase in temperature matters, *Science*, 379, 78–83, <https://doi.org/10.1126/science.abo1324>, 2023.
- Rowan, A. V., Egholm, D. L., Quincey, D. J., and Glasser, N. F.: Modelling the feedbacks between mass balance, ice flow and debris transport
 430 to predict the response to climate change of debris-covered glaciers in the Himalaya, *Earth and Planetary Science Letters*, 430, 427–438, <https://doi.org/10.1016/j.epsl.2015.09.004>, 2015.
- Rowan, A. V., Nicholson, L. I., Quincey, D. J., Gibson, M. J., Irvine-Fynn, T. D., Watson, C. S., Wagnon, P., Rounce, D. R., Thompson, S. S., Porter, P. R., et al.: Seasonally stable temperature gradients through supraglacial debris in the Everest region of Nepal, Central Himalaya, *Journal of Glaciology*, 67, 170–181, <https://doi.org/10.1017/jog.2020.100>, 2021.
- 435 Scherler, D., Wulf, H., and Gorelick, N.: Global assessment of supraglacial debris-cover extents, *Geophysical Research Letters*, 45, 11–798, <https://doi.org/10.1029/2018GL080158>, 2018.
- Shugar, D. H. and Clague, J. J.: The sedimentology and geomorphology of rock avalanche deposits on glaciers, *Sedimentology*, 58, 1762–1783, <https://doi.org/10.1111/j.1365-3091.2011.01238.x>, 2011.

- Thakuri, S., Salerno, F., Smiraglia, C., Bolch, T., D'Agata, C., Viviano, G., and Tartari, G.: Tracing glacier changes since the 1960s
440 on the south slope of Mt. Everest (central Southern Himalaya) using optical satellite imagery, *The Cryosphere*, 8, 1297–1315,
<https://doi.org/10.5194/tc-8-1297-2014>, 2014.
- Thomas, J. W.: *Numerical partial differential equations: finite difference methods*, Springer Science & Business Media, 2013.
- Tielidze, L. G., Bolch, T., Wheate, R. D., Kutuzov, S. S., Lavrentiev, I. I., and Zemp, M.: Supra-glacial debris cover changes in the Greater
Caucasus from 1986 to 2014, *The Cryosphere*, 14, 585–598, <https://doi.org/10.5194/tc-14-585-2020>, 2020.
- 445 Zhang, T. and Osterkamp, T.: Considerations in determining thermal diffusivity from temperature time series using finite difference methods,
Cold Regions Science and Technology, 23, 333–341, [https://doi.org/doi.org/10.1016/0165-232X\(94\)00021-O](https://doi.org/doi.org/10.1016/0165-232X(94)00021-O), 1995.